

Leukocyte functional antigen 1 lowers T cell activation thresholds and signaling through cytohesin-1 and Jun-activating binding protein 1

Omar D Perez^{1,2}, Dennis Mitchell¹, Gina C Jager¹, Sharon South¹, Chris Murriel³, Jacqueline McBride⁴, Lee A Herzenberg⁵, Shigemi Kinoshita⁶ & Garry P Nolan^{1,2}

Leukocyte functional antigen 1 (LFA-1), with intercellular adhesion molecule ligands, mediates T cell adhesion, but the signaling pathways and functional effects imparted by LFA-1 are unclear. Here, intracellular phosphoprotein staining with 13-dimensional flow cytometry showed that LFA-1 activation induced phosphorylation of the β_2 integrin chain and release of Jun-activating binding protein 1 (JAB-1), and mediated signaling of kinase Erk1/2 through cytohesin-1. Dominant negatives of both JAB-1 and cytohesin-1 inhibited interleukin 2 production and impaired T helper type 1 differentiation. LFA-1 stimulation lowered the threshold of T cell activation. Thus, LFA-1 signaling contributes to T cell activation and effects T cell differentiation.

Adhesion between T cells and antigen-presenting cells (APCs) is necessary for the formation of the immunological synapse and is mediated by T cell surface molecules, including leukocyte functional antigen 1 (LFA-1, also known as CD11a and CD18) and the intercellular adhesion molecule (ICAM) ligands¹. Engagement of the T cell receptor (TCR) with a recognized complex of peptide–major histocompatibility complex (MHC) protein on APCs is necessary for *in vivo* T cell activation. T cell costimulatory surface molecules such as CD28 and CD2 (LFA-2), and their APC counter-receptors B7 (CD80-86) and CD58 (LFA-3), initiate and regulate T cell activation².

In contrast to the extensive data available concerning signals involved in TCR and CD28 ligation, much less is known about specific signals generated by adhesion-mediated events involved in the contact of T cells with APCs. Optimal proliferation of T cells and enhancement of interleukin 2 (IL-2) production requires adhesive interactions between costimulatory receptors on T cells and their counter-ligands on APCs. In addition to TCR and CD28 stimulation, model systems used to study T cell activation have shown that increasing antigen density by more than 10,000-fold does not initiate naive CD4⁺ T cell proliferation or cytokine synthesis in the absence of ICAM–LFA-1 interaction^{3,4}. ICAM–LFA-1 interactions may provide stronger adhesion that facilitates more pronounced signaling through other ligand-receptor pairs. Despite indications that ICAM–LFA-1 interactions can lead to sustained intracellular calcium response, increased inositol phospholipid hydrolysis and the appearance of the hyperphosphorylated p23 form of the TCR ζ chain^{4,5,6}, the specific functional consequences of an LFA-1-mediated ‘costimulatory’ signal are not well defined. LFA-1 signals to

the JNK pathway through JAB-1 (ref. 7) and involvement of cytohesin-1 in downstream signals (a regulator of LFA-1 activation)⁸, indicating that intracellular events are important for LFA-1 function. These studies indicate that the ICAM–LFA-1 interaction is capable of initiating costimulatory T cell signaling events.

Intracellular phosphoprotein epitope staining has allowed the simultaneous monitoring of multiple active kinases, target phosphorylation sites and surface phenotypes with up to 13 parameters by flow cytometry in single cells⁹. Using phosphoprotein profiling in conjunction with surface immunophenotyping and cytokine bead arrays, we show here that human naive T cells (CD3⁺CD4⁺CD8⁻CD62L⁺CD45RA⁺CD11a^{dim}CD27⁺CD28⁺) were optimally activated after simultaneous stimulation with CD3, CD28 and LFA-1. The integration of signaling pathways from CD3, CD28 and LFA-1 activated multiple pathways (the MAPK, PKC, phospholipase- γ and Src kinases), which correlated with cell cycle entry and expression of IL-2, CD25 and CD69. This cell-based proteomic approach allowed for differential analysis of phosphoproteins as induced by stimulation of CD3, CD28 and LFA-1 individually and in combination.

LFA-1 stimulation induced PKC- δ -dependent phosphorylation of the β_2 integrin chain, an event that corresponded with the release of JAB-1 from LFA-1, and activation of activator protein-1 (AP-1)-driven transcription. We also identified cytohesin-1-mediated Erk1/2 (also referred to as p42/44 MAPK) activation that was independent of JAB-1 signaling. Using dominant negative peptides against JAB-1 and cytohesin-1, we inhibited LFA-1-induced c-Jun phosphorylation and cytohesin-1 activation of the Erk1/2 pathway, respectively. This

¹Department of Microbiology and Immunology, ²The Baxter Laboratory of Genetic Pharmacology, and the Departments of ³Molecular Pharmacology, ⁴Immunology and Rheumatology and ⁵Genetics, Stanford University School of Medicine, Stanford, California 94305, USA. ⁶Department of Dermatology, Center for Immunology, The University of Texas Southwestern Medical Center, 5323 Harry Hines Boulevard, Dallas, Texas 75390-9069, USA. Correspondence should be addressed to G.P.N. (gnolan@stanford.edu).

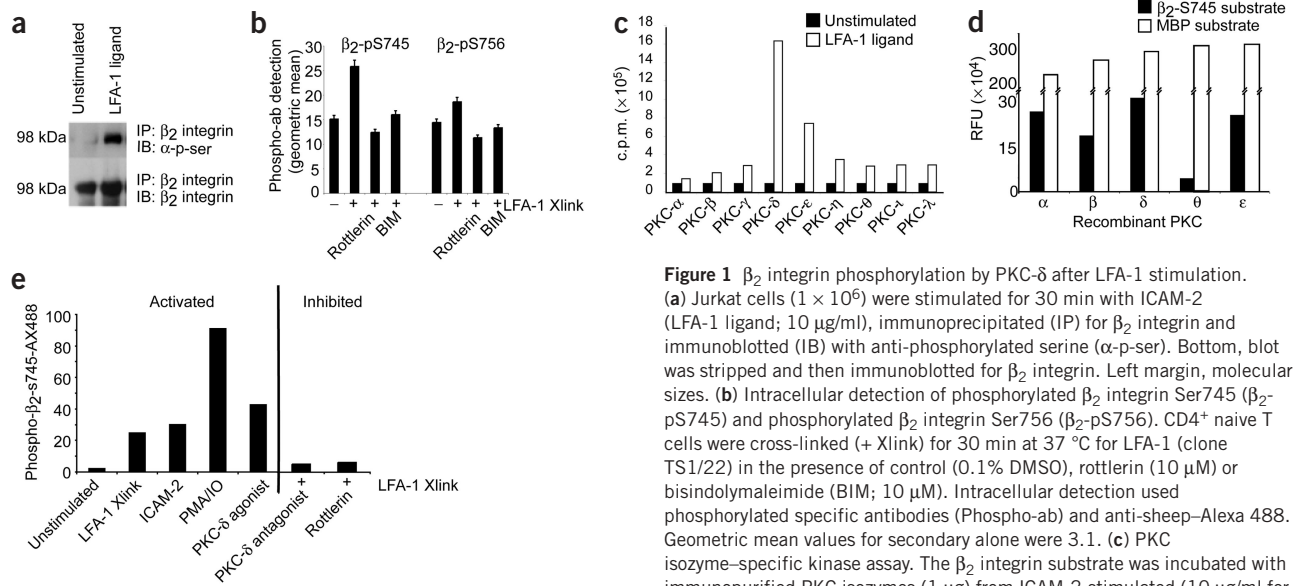


Figure 1 β_2 integrin phosphorylation by PKC- δ after LFA-1 stimulation. (a) Jurkat cells (1×10^6) were stimulated for 30 min with ICAM-2 (LFA-1 ligand; 10 μ g/ml), immunoprecipitated (IP) for β_2 integrin and immunoblotted (IB) with anti-phosphorylated serine (α -p-ser). Bottom, blot was stripped and then immunoblotted for β_2 integrin. Left margin, molecular sizes. (b) Intracellular detection of phosphorylated β_2 integrin Ser745 (β_2 -pS745) and phosphorylated β_2 integrin Ser756 (β_2 -pS756). CD4⁺ naive T cells were cross-linked (+ Xlink) for 30 min at 37 $^{\circ}$ C for LFA-1 (clone TS1/22) in the presence of control (0.1% DMSO), rottlerin (10 μ M) or bisindolymaleimide (BIM; 10 μ M). Intracellular detection used phosphorylated specific antibodies (Phospho-ab) and anti-sheep-Alexa 488. Geometric mean values for secondary alone were 3.1. (c) PKC isozyme-specific kinase assay. The β_2 integrin substrate was incubated with immunopurified PKC isozymes (1 μ g) from ICAM-2-stimulated (10 μ g/ml for

30 min) or unstimulated cells in the presence of [γ - 32 P]ATP. (d) Recombinant PKC isozyme kinase assay with the β_2 integrin Ser745 peptide (β_2 -S745) and myelin basic protein (MBP) substrates. Phosphorylation was assessed by anti-phosphorylated serine ELISA (for β_2 -S745) or anti-phosphorylated MBP-horseradish peroxidase ELISA (for MBP). Relative fluorescent units (RFU) were quantified and normalized for kinase 'blank' (negative) controls. (e) Intracellular detection of phosphorylated β_2 integrin Ser745 peptide substrate in human CD4⁺ T cells that were LFA-1 cross-linked (+ Xlink) and treated with ICAM-2 (10 μ g/ml), phorbol 12-myristate 13-acetate (500 ng/ml) plus ionomycin (1 μ M), PKC- δ agonist peptide (1 μ M), PKC- δ antagonistic peptide (1 μ M) or rottlerin (10 μ M). Cross-linking treatments were for 30 min at 37 $^{\circ}$ C, and cells were incubated for 15 min at 37 $^{\circ}$ C with inhibitory agents before LFA-1 cross-linking. Data represent geometric mean values for fluorescence signals.

impaired IL-2 production and development of T helper type 1 (T_H1) cells producing interferon- γ (IFN- γ). LFA-1 stimulation increased sensitivity to costimulation with CD3 and CD28, led to greater IL-2 production at much earlier time points, induced more robust mitogenic progression and polarized T cell differentiation toward T_H1 cells. Thus, the additional LFA-1 signals can contribute functionally both to T cell activation and to effector cell differentiation.

RESULTS

ICAM-2 induces phosphorylation of LFA-1

LFA-1 integrin activation requires a conformational change that can be induced by TCR cross-linking or phorbol ester treatment¹⁰. We sought to distinguish signaling events that were unique to LFA-1 and independent of TCR signaling. Using a soluble LFA-1 ligand (ICAM-2) on Jurkat cells, we noted serine phosphorylation of β_2 integrin (Fig. 1a). We reproducibly found that this serine phosphorylation occurred after phorbol ester treatment (an activator of PKC; data not shown), and we therefore sought to identify both the β_2 integrin phosphorylation sites and which PKC isozymes were responsible for the β_2 integrin phosphorylation after LFA-1 stimulation *in vivo*. The serine residue at position 745 (Ser745) and threonine residues at positions 758, 759 and 760 are phosphorylated by multiple PKC isozymes *in vitro*¹¹. We confirmed the intracellular phosphorylation of β_2 integrin Ser745 and Ser756 by flow cytometry in naive CD4⁺ T cells with phospho-specific antibodies to phosphorylated Ser745 and phosphorylated Ser756 peptides⁹. Stimulation by LFA-1 cross-linking produced increased phosphorylated β_2 integrin Ser745; this was inhibited by both the PKC- δ -specific inhibitor rottlerin and the general PKC inhibitor bisindolymaleimide (Fig. 1b, lanes 2 with 3 versus 4). We did not detect an increase in phosphorylated β_2 integrin Ser756 after LFA-1 cross-linking; however, amounts were slightly decreased after

treatment with rottlerin or bisindolymaleimide (Fig. 1b, lanes 5–8). We confirmed these results by phosphorylated serine-based enzyme-linked immunosorbent assay (ELISA) of peptides corresponding to the β_2 integrin cytoplasmic domain (data not shown). The kinase that phosphorylates Ser756 has not been identified and at least *in vitro* is not a PKC isozyme, although its phosphorylation has been reported to be dependent on PKC¹¹.

To assess if PKC isozymes could phosphorylate β_2 integrin after LFA-1 stimulation, we immunopurified β_2 integrin from unstimulated Jurkat cells and used this as a substrate in a PKC isozyme-specific kinase assay. We immunoprecipitated PKC isozymes α , β , γ , δ , ϵ , η , θ , ι and λ from both LFA-1-stimulated and unstimulated Jurkat cells, and used these in a radioactive kinase assay with the purified β_2 integrin as substrate, along with myelin basic protein as a control to measure total incorporation of phosphorylation. PKC- δ from activated Jurkat cells strongly phosphorylated β_2 integrin (Fig. 1c, lane 5). Some phosphorylation was induced by PKC- ϵ , and lower levels of phosphorylation were detected by the other PKC isozymes.

Because β_2 integrin may be phosphorylated at more than one site and additional substrates could have been immunoprecipitated, although undetected, with the β_2 integrin (Fig. 1c), we tested whether recombinant human PKC isozymes α , β , δ , ϵ , η , θ , ι and λ were able to phosphorylate *in vitro* a synthesized β_2 integrin peptide corresponding to residues 740–750 of the β_2 integrin cytoplasmic region (called β_2 -pep745 here; CKEKLKSQWNNND-biotin). Using PKC isozyme kinase assays on plate-bound β_2 -pep745, we detected phosphorylation by anti-phosphoserine-based ELISA. Recombinant PKC- α , PKC- β , PKC- δ and PKC- ϵ phosphorylated β_2 integrin at Ser745 (Fig. 1d). Recombinant PKC- θ did not phosphorylate the β_2 integrin Ser745 substrate (Fig. 1d). PKC- α , PKC- β , PKC- δ , PKC- θ and PKC- ϵ efficiently phosphorylated the general PKC substrate myelin basic

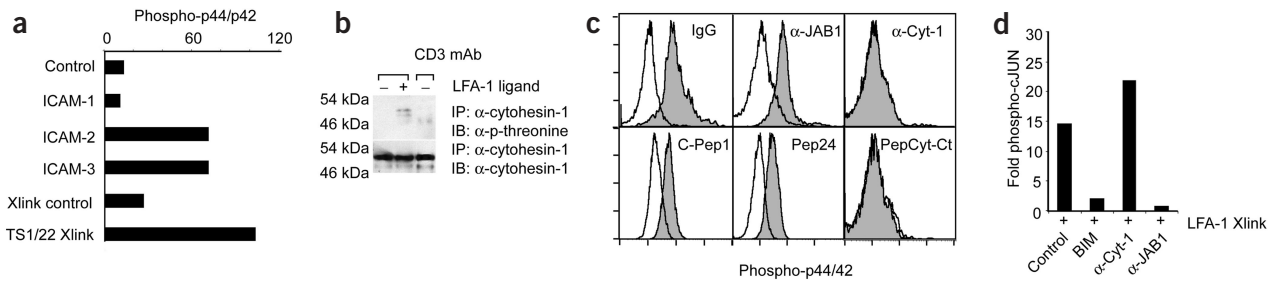


Figure 3 LFA-1 signals Erk1/2 MAPK. (a) Intracellular induction of phosphorylated Erk1/2 (Phospho-Erk1/2) after LFA-1 stimulation. Jurkat cells were deprived of serum for 12 h and incubated for 30 min with stimuli of ICAM-1, ICAM-2 or ICAM-3 fusion proteins (10 μ g/ml), or were LFA-1 cross-linked (with clone TS1/22). Cells were analyzed for intracellular phosphorylated Erk1/2 by flow cytometry; data represent geometric mean fluorescence intensities. (b) Phosphorylated threonine immunoblot (IB) of cytohesin-1 immunoprecipitated (IP) from LFA-1 ligand-treated (10 μ g/ml for 30 min) or CD3 cross-linked T cells. α -, anti-; p-, phosphorylated. Left margin, molecular sizes. (c) Assessment of phosphorylated Erk1/2 in cells loaded with immunoglobulin G (IgG), anti-JAB-1 (α -JAB-1), anti-cytohesin-1 C terminus (α -Cyt-1), and the C-terminal peptide of cytohesin-1 (pepCyt-Ct) after LFA-1 cross-linking. Antibodies and peptides were transfected at 1 μ g and detected with phosphorylated Erk1/2–Alexa 488. Detection of cells containing the control peptide C-Pep1 or Pep24 used phosphorylated Erk1/2–phycoerythrin. (d) Detection of intracellular phosphorylated c-Jun (phospho-cJun) in cells transfected with 10 μ M bisindolymaleimide (BIM), 1 μ g anti-cytohesin-1 C terminus (α -Cyt-1) or 1 μ g anti-JAB-1 (α -JAB-1) after LFA-1 cross-linking. Phosphorylation was assessed with anti-phospho-Jun–Alexa 633 and is presented as ‘fold phosphorylation’ relative to that of control cells. Xlink, cross-link.

a control peptide had no effect after the induction of phosphorylated c-Jun (Fig. 2f, lanes 1 and 2). These data indicate that disassociation of JAB-1 from LFA-1 is induced by phosphorylation at Ser745 and mediates LFA-1-dependent c-Jun activation and subsequent AP-1 activity.

LFA-1 signals to Erk1/2 MAPK through cytohesin-1

As AP-1 activity requires expression of c-Fos, a target of the Erk1/2 pathway, LFA-1 may induce other signals that can activate molecules such as Erk1/2, leading to c-Fos induction. A series of kinase profiling experiments showed that LFA-1 ligands ICAM-2 and ICAM-3, as well as LFA-1 cross-linking with monoclonal antibodies, induced phosphorylation of Erk1/2 in Jurkat cells (Fig. 3a). This did not occur with soluble ICAM-1 (Fig. 3a), strongly indicating a distinction between the ICAMs and how they signal through LFA-1. We confirmed these results by Erk1/2 ‘phosphorylation immunoblotting’ and Erk1/2 activity assays (data not shown).

With a series of genetic, biochemical and pharmacological screens, we identified a requirement for GTPase activity for LFA-1 signaling to the Erk1/2 pathway in Jurkat cells (data not shown). Cytohesin-1 is an LFA-1-interacting protein that regulates LFA-1 adhesion to ICAM-1 and is a guanine nucleotide-exchange factor for ADP-ribosylation factor GTPases¹³. As phosphorylation of cytohesin-1 at threonine is important for mediation of LFA-1 adhesion¹⁴, we first assessed whether cytohesin-1 threonine phosphorylation was induced after stimulation by an LFA-1 ligand. Treatment with ICAM-2 induced detectable threonine phosphorylation in cytohesin-1, an effect that did not occur with CD3 cross-linking of Jurkat cells (Fig. 3b), indicating that LFA-1 may signal through cytohesin-1.

To confirm that cytohesin-1 functioned in the LFA-1–Erk1/2 signaling pathway, we used a *trans* dominant negative polypeptide derived from cytohesin-1 to block its function⁸. We synthesized a C-terminal peptide corresponding to this region and delivered it intracellularly to Jurkat cells. Delivery of either the cytohesin-1 C-terminal–blocking polypeptide or an antibody to the C terminus of cytohesin-1 inhibited LFA-1 induction of Erk1/2 phosphorylation (Fig. 3c, right). Delivery of an antibody to JAB-1 (anti-JAB-1) or control immunoglobulin G, or intracellular expression of a control peptide and Pep24 (the JAB-1 antagonist), did not affect the LFA-1 induction of Erk1/2 (Fig. 3c). To confirm that the cytohesin-1 pathway was distinct from the JAB-1-mediated c-Jun pathway, we used the same treatment and monitored

phosphorylated c-Jun as a ‘readout’ of LFA-1 stimulation by flow cytometry. Inhibition of all PKC isozymes with bisindolymaleimide blocked LFA-1-mediated c-Jun phosphorylation, as expected (Fig. 3d). Delivery of anti-cytohesin-1 did not affect the signal, whereas delivery of anti-JAB1 completely blocked LFA-1-mediated c-Jun phosphorylation (Fig. 3d). These results identified cytohesin-1 as a mediator of LFA-1-induced Erk1/2 phosphorylation, a pathway distinct from LFA-1-mediated JAB-1 c-Jun-activating events. Therefore, cytohesin-1 links LFA-1 to protein complexes that, in turn, signal Erk1/2.

Kinase phosphoprotein profiling of costimulatory signaling

Next, we determined the contribution of LFA-1 signaling to the CD3–CD28 ‘cosignal’ by quantitative kinetic analyses of multiple active kinases by flow cytometry on naive CD4⁺ T cells. We computed the difference in signaling as the logarithm of the geometric mean of the ‘phospho-signatures’ for the stimulus of CD3, CD28 and LFA-1 relative to the geometric mean of the ‘phospho-signatures’ for the stimulus of CD3 plus CD28, and color coded the ‘fold intensity’ for time-referenced experiments (Fig. 4). We acquired 1×10^4 naive CD4⁺ T cells for each data point. We computed phosphoprotein induction profiles and clustered them with techniques similar to those used for microarray gene expression analysis. We monitored kinetic analyses of the phosphorylation of the kinases PLC- γ 1, Lck, AKT, ELK-1, SRC, p38, RAF-1 and Erk1/2, and phospholipids PIP₃ and PIP₂, compared these in naive T cells stimulated for CD3, CD28 and LFA-1 or CD3 and CD28. We determined the relative fold induction (CD3, CD28 and LFA-1 versus CD3 and CD28) of phosphorylation of each of these kinases (Fig. 4).

An increase in PI3 kinase activity, as determined by PIP₃ production, in naive T cells 5 min after stimulation of CD3, CD28 and LFA-1 versus stimulation of CD3 and CD28 corresponded with the expected increase in phosphorylated PLC- γ 1 at 10 min (Fig. 4, green). We confirmed enhanced phosphorylation of the Erk1/2 pathway (RAF-1, Erk1/2 and ELK-1) for LFA-1 signaling (Fig. 4). There was an enhancement of Src and JNK phosphorylation in the presence of LFA-1 signaling (Fig. 4). There was little apparent contribution to p38, pAKT, pLck or PIP₂ phosphorylation imparted by the addition of LFA-1 signaling, results consistent with the idea that costimulation with CD3 plus CD28 is optimal for these phospho-epitopes (Fig. 4). The phosphorylated kinases MEK and RAF showed matched slight upregulation at 5 min with a downward trend at 30 min and an eventual return to no increased signaling

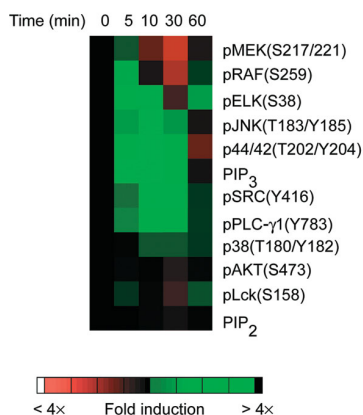


Figure 4 Differential active kinase profiling by flow cytometry. Kinetic analysis of phosphoproteins (p) after a single stimulation with anti-CD3 plus anti-CD28, with and without ICAM-2, in human naive CD4⁺ T cells by differential display of flow cytometric phosphoprotein signatures. Ratios of the fluorescent phosphoprotein antibodies (left margin) were calculated from the following equation (GMFI is geometric mean fluorescent intensity): $\text{Log} [(GMFI_{CD3-CD28-LFA-1}) / (GMFI_{CD3-CD28})]$. 'Fold phosphorylation' is indicated by the color intensity scale (bottom): red, high; green, low. p44/42, Erk1/2.

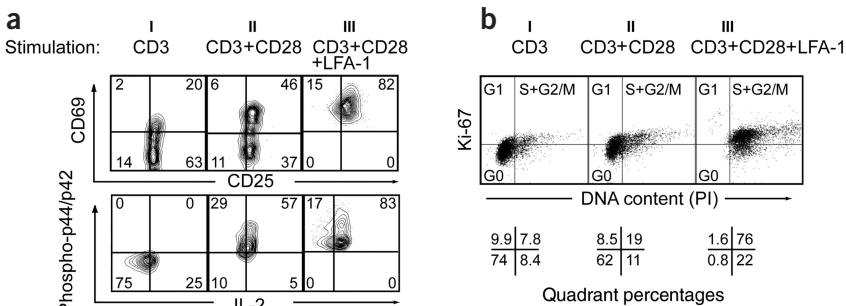
imparted by either the double- or triple-stimulation regimen.

The kinetics of the phosphorylation 'signatures' indicate that both quantitative and qualitative differences in signaling through multiple kinases are present after addition of the LFA-1 signal, indicating that LFA-1 signaling cooperates with stimulation of CD3 and CD28 to augment phosphorylation and dephosphorylation events. The increased intensity in Erk1/2 has substantial consequences for T cell activation kinetics (discussed below).

LFA-1 promotes T cell activation and mitotic progression

Given the activation of signaling cascades described above, we determined the functional outcome of LFA-1 signaling after naive T cell activation with costimulation of CD3 and CD28. We 'combined' magnetic-activated cell sorting and 13-dimensional multiparameter flow cytometry (surface immunophenotyping, intracellular production of active kinases and cytokines) with profiling of secreted cytokines (cytometric bead arrays) to obtain a more complete assessment of T cell activation and effector cell function (Supplementary Fig. 2 online). We cross-referenced these data sets for correlatives of cell surface receptor activation, intracellular signaling and functional outcomes.

Figure 5 Multidimensional analysis of naive CD4⁺ T cells. Magnetic cell sorting, 13-parameter flow cytometry, transcription factor profiling and cytokine bead arrays were 'combined' to determine the effect of stimulation on immunophenotyped naive CD4⁺ T cells (CD3⁺CD4⁺CD8⁻CD45RA⁺CD62L⁺CD11a^{dim}CD27⁺CD28⁺). (a) Intracellular IL-2 and phosphorylated Erk1/2 (Phospho-Erk1/2) were correlated with surface phenotype and activation markers CD69 and CD25. Numbers in quadrants indicate percentages of each population. (b) Cell cycle analysis of CD4⁺ T cells stimulated with CD3, CD3 plus CD28, or CD3, CD28 and LFA-1 ligand. Cells in the G0, G1, and S + G2/M phases of the cell cycle were determined by double staining for expression of Ki-67 and DNA content (propidium iodide; PI). Low Ki-67⁻ signals were considered cells in G0; Ki-67⁺ signals with 2n DNA, cells in G1; and Ki-67⁺ signals with >2n DNA, cells in S or G2/M.



We achieved enrichment of primary naive T cells by magnetic-activated cell sorting (negative depletion) with markers CD8, CD19, CD16, CD14, HLA-DR and CD44 to remove cytotoxic T cells, B cells, natural killer cells, macrophages and activated T cells, from peripheral blood mononuclear cell samples. We used eight markers to identify naive human T cells (CD3⁺CD4⁺CD8⁻CD45RA⁺CD62L⁺CD11a^{dim}CD27⁺CD28⁺). We stimulated CD3, CD28 and LFA-1 separately and in combination to stimulate these enriched nonactivated T cells. We analyzed mature naive T cells, as determined by the eight immunophenotypic markers, for CD69, CD25 and IL-2 expression simultaneously by 13-dimensional flow cytometry, as expression of these markers defines an activated T cell^{15,16}. We analyzed samples at 8, 12 and 24 h after stimulation to monitor the phosphorylation levels of stimulated cells. At 8 h after stimulation, CD3 stimulation alone induced minor CD69 activation and small amounts of phosphorylated Erk1/2 (Fig. 5a, I). Stimulation of CD3 plus CD28 induced more CD69 activation, activated phosphorylated Erk1/2 and stimulated IL-2 production (Fig. 5a, II). However, naive T cells were optimally activated (CD3⁺CD4⁺CD8⁻CD45RA⁺CD62L⁺CD11a^{dim}CD27⁺CD28⁺) in the presence of LFA-1 plus CD3 and CD28 at 8 h (Fig. 5a, III). The addition of the LFA-1 ligand to CD3 plus CD28 stimulation, produced more CD69 and CD25 expression than did stimulation of CD3 plus CD28 (81.5% versus 45.8% CD69⁺CD25⁺ naive T cells). Intracellular amounts of phosphorylated Erk1/2 and IL-2 production were also higher in naive CD4⁺ T cells (Fig. 5a, III). Although we found CD25 and IL-2 expression after stimulation of CD3 and CD28, the amounts and frequency of naive T cells that were CD69⁺CD25⁺IL-2⁺ were greater in the cells stimulated with CD3, CD28 and LFA-1 (Fig. 5a, III).

T cell activation requires cell cycle entry and subsequent cell proliferation, which is an important 'downstream' outcome of cellular activity induced by signal transduction pathways. We measured cellular proliferation and concomitant cell cycle initiation by flow cytometry staining for DNA content and Ki-67 proliferation antigen. Cell cycle entry after 12 h of stimulation with CD3, CD28 and LFA-1 was indicated by DNA content >2n and expression of nuclear antigen Ki-67 (Fig. 5b). Proliferation-associated antigen Ki-67 and total DNA content quantify the cells in different cell cycle phases. Stimulation with CD3, CD28 and LFA-1 produced a higher percentage (76%) of cells in the S and G2/M phase than did stimulation with CD3 and CD28 (19%, versus only 7.8% with CD3 alone; Fig. 5b). Thus, there was a more profound induction cell cycle entry in cells stimulated with CD3, CD28 and LFA-1 than in cells stimulated with CD3 and CD28.

We quantified IL-2 secretion by cytometric bead array. At the initial 6-hour time point, stimulation with CD3, CD28 and LFA-1 produced

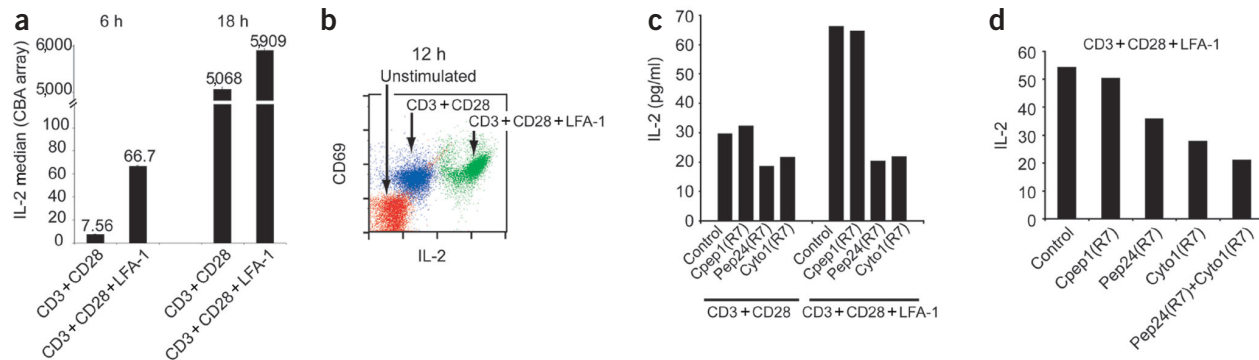


Figure 6 T cell activation assessed by IL-2, and surface CD25 and CD69 markers. (a) Cytometric bead array (CBA) measurements of secreted IL-2 production after 6 or 18 h of stimulation. The mean fluorescence intensity (MFI) of beads corresponding to IL-2 detection was computed and plotted. (b) Bivariate plot of CD69 expression and intracellular detection of IL-2. Cells were left unstimulated, or were stimulated for 6 h with CD3 plus CD28, or CD3, CD28 and LFA-1 and then stimulated for an additional 6 h in the presence of brefeldin-A before being processed for intracellular staining. (c) Naive T cells (1×10^6) were pre-incubated for 15 min with cytohesin-1 dominant negative peptide (Cyto1), Pep24, control peptide (Cpep1) or a control carrier peptide at a concentration of 5 μ M, and were transferred to plates coated with CD3 and CD28 (left) or CD3, CD28 and LFA-1 (right). IL-2 secretion was measured by cytometric bead array at 10 h and quantified with a standard calibration curve with recombinant IL-2. (d) Naive T cells (1×10^6) were pre-incubated for 15 min with Pep24, Cyto1, Cpep1, Pep24 plus Cyto1, or a control carrier peptide, and were surface cross-linked for CD3, CD28 and LFA-1. Intracellular IL-2 was assessed by flow cytometry after 6 h of stimulation. R7 (c,d), hepta-arginine tag. Data represent geometric mean values.

an approximately ninefold increase in IL-2 secretion compared with stimulation by CD3 plus CD28 (Fig. 6a). At 18 h after stimulation, stimulation by CD3 and CD28 induced increased soluble IL-2; however, the amounts were still lower than with stimulation with CD3, CD28 and LFA-1 (Fig. 6a). To distinguish the differences in IL-2 production after stimulation with CD3 plus CD28 and stimulation with CD3, CD28 and LFA-1, we used titration and kinetic analyses for stimulus-induced T cell activation, as assessed by intracellular IL-2 production and CD25 and CD69 surface expression by flow cytometry. At 6 h after stimulation, we blocked cytokine secretion with brefeldin-A and allowed cytokines to accumulate for an additional 6 h. Stimulation with CD3, CD28 and LFA-1 induced more intracellular IL-2 at 12 h than did the other stimuli regimens (Fig. 6b). Therefore, LFA-1 signaling in stimulation with CD3 plus CD28 results in early IL-2 production.

Activity of Erk1/2 is necessary for T cell activation and subsequent IL-2 production^{17,18}. As LFA-1 signals through cytohesin-1 to activate the Erk1/2 pathway, and this was effectively blocked by a cytohesin-1 dominant negative peptide (Fig. 3d), we tested whether blocking cytohesin-1 would abrogate the LFA-1 contribution to IL-2 production in naive human T cells. We stimulated T cells for 24 h on plates coated with antibodies to CD3, CD28 and LFA-1 in the presence of increasing concentrations of the cell-permeable cytohesin-1 dominant negative peptide. IL-2 production was inhibited in a dose-dependent way. We delivered the cell-permeable JAB-1 antagonistic peptide Pep24 and the cytohesin-1 peptide into naive T cells, and monitored IL-2 production 10 h after stimulation with CD3 plus CD28 or with CD3, CD28 and LFA-1. This time point was necessary, as earlier time points did not induce IL-2 after stimulation with CD3 and CD28 (Fig. 6a). Pep24 and the cytohesin-1 peptide inhibited IL-2 production in naive T cells stimulated with CD3, CD28 and LFA-1 (Fig. 6c). Both peptides also inhibited IL-2 production in cells stimulated with CD3 plus CD28, although the amounts of control cells were lower than those of cells stimulated with CD3, CD28 and LFA-1 (Fig. 6c). We tested whether the inhibition of IL-2 synthesis was greater with combinations of peptides. We monitored intracellular production of IL-2 at 6 h in cells stimulated with CD3, CD28 and LFA-1. Both Pep24 and the cytohesin-1 peptide blocked the production of intracellular IL-2 (Fig. 6d) at levels similar to those noted for secreted IL-2 (Fig. 6c). Stimulation

with CD3 plus CD28 resulted in IL-2 amounts similar to those of cells stimulated with CD3, CD28 and LFA-1 at 6 h when either JAB-1 or cytohesin-1 was inhibited (Fig. 6c). There was slight inhibition of IL-2 production after stimulation with CD3 plus CD28 when JAB-1 or cytohesin-1 was inhibited (Fig. 6c). The combination of the JAB-1 antagonist and the cytohesin-1 antagonist peptide inhibited IL-2 synthesis to a greater extent than either peptide alone (Fig. 6d). Thus, inhibition of either JAB-1 or cytohesin-1 is sufficient to limit the contribution of LFA-1 to CD3 plus CD28 'cosignaling' at early time points during T cell activation, but not as well as at later time points.

LFA-1 polarizes toward a T_H1 phenotype

It is apparent from the data above that LFA-1 signaling in conjunction with CD3 plus CD28 leads to substantial differences in T cell kinase phosphoprotein status, in mitotic progression and in the expression of known surface markers associated with commitment. To determine the effector phenotype outcomes contributed by LFA-1 'cosignaling', we did titration experiments of stimulation with CD3 versus CD28 as well as CD3 plus CD28 versus LFA-1, and monitored intracellular production of IL-4 and IFN- γ . Activated CD4⁺ T cells differentiate into T_H1 or T_H2 effector T cells and can be preferentially directed toward either pathway by cytokines or additional stimuli. Effector cells can be identified by their cytokine secretion profile. T_H1 cells are characterized by high IFN- γ and low IL-4, whereas T_H2 cells are characterized by high IL-4 and low IFN- γ ¹⁹. Monitoring of intracellular IFN- γ in CD4⁺ naive T cells indicated that the frequency of CD4⁺IFN- γ ⁺ (immunophenotyped with eight markers) was greater after 24 h in cell populations stimulated with CD3, CD28 and LFA-1 than in those stimulated with CD3 plus CD28 (Fig. 7a). We used cytometric bead arrays to assess the secretion of IFN- γ and IL-4 in naive T cells after 18 h of stimulation. We computed the mean of the detected bound soluble cytokines, and plotted this as a ratio of IFN- γ to IL-4. Stimulation with CD3, CD28 and LFA-1 induced a higher ratio of secreted IFN- γ to IL-4 than did stimulation with CD3 plus CD28 at 18 h (Fig. 7b). We found no cytokine induction in cells stimulated with CD3, CD28 or LFA-1 alone (data not shown). We then monitored the intracellular production of IFN- γ and IL-4 at an earlier time point and across multiple titrations. Computation of the ratio of

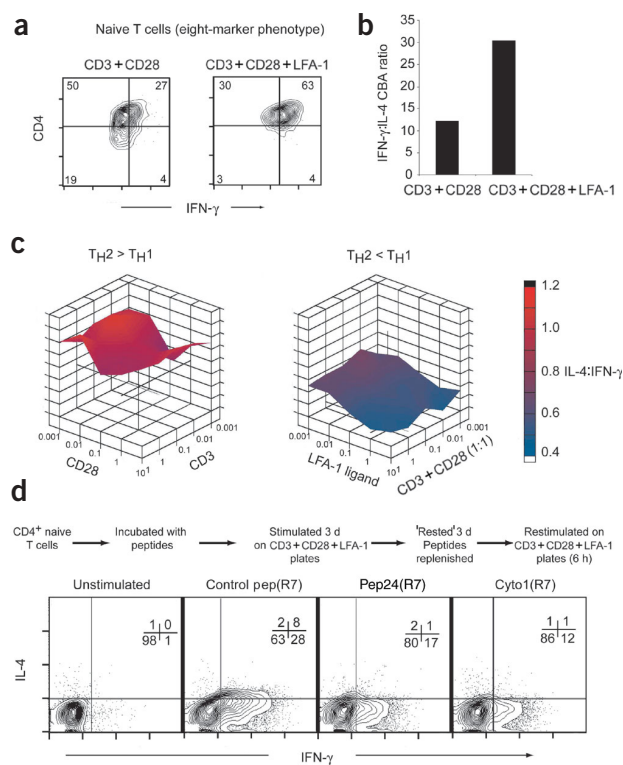


Figure 7 Production of IL-4 and IFN- γ in human naive CD4⁺ T cells in response to stimulation with CD3 plus CD28 or with CD3, CD28 and ICAM-2. **(a)** Intracellular detection of IFN- γ in naive CD4⁺ T cells (eight-marker phenotype; CD3⁺CD4⁺CD8⁻CD62L⁺CD45RA⁺CD11a^{dim}CD27⁺CD28⁺) after 24 h of stimulation with CD3 and CD28 (left) or CD3, CD28 and ICAM-2 (right). Cells are gated for all native T cell markers and are shown as CD4⁺ and IFN- γ . Brefeldin-A (10 μ g/ml) was added at 18 h before samples were processed for intracellular staining. Numbers in quadrants indicate percentages of each population. **(b)** Cytometric bead array (CBA) for the ratio of secreted IFN- γ and IL-4 after 16 h of stimulation with CD3 plus CD28 (10 μ g/ml; left) or CD3, CD28 and ICAM-2 (10 μ g/ml; right). Values were simultaneously measured in the supernatants of treated cells by CBA and computed as a ratio of IFN- γ to IL-4. **(c)** Intracellular IFN- γ and IL-4 after 6 h of stimulation with titrations of CD3 versus CD28 (left) or CD3 plus CD28 versus LFA-1 (right). Median fluorescence values were normalized to those of unstimulated cells, and log ratios of IL-4 to IFN- γ were computed and plotted as intensity contour plots. Intensity is shown in the range indicator (far right). **(d)** Frequency of IFN- γ -producing T_H1 cells after JAB-1 and cytohesin-1 inhibition. CD4⁺ naive T cells were loaded with JAB-1 or cytohesin-1 antagonistic peptides (Pep24 and Cyto1, respectively), or with control carrier peptides (Control pep), stimulated for 3 d on plates coated with CD3, CD28 and LFA-1, allowed to 'rest' for 3 d, and then assessed for intracellular IFN- γ and IL-4 production. Data represent IL-4 and IFN- γ expression. Peptides and media were replenished every 3 d. Numbers in quadrants indicate percentages of each population. R7 (c,d), hepta-arginine tag.

the median fluorescence of intracellular IL-4 to that of IFN- γ showed that the LFA-1 stimulus, at all concentrations tested, favored a low ratio of IL-4 to IFN- γ (Fig. 7c). Therefore, in the absence of additional stimulants, LFA-1 signaling polarized T cells toward a T_H1 phenotype. This may be a direct effect of LFA-1 costimulation or it could occur through autocrine activation of the transcription factor STAT1 after cognate cytokine secretion.

We sought to assess functionally whether inhibition of JAB-1 or cytohesin-1 affected the development of IFN- γ -secreting T_H1 cells in long-term culture stimulated in the presence of LFA-1 stimulation. We assessed IFN- γ production in cells stimulated with CD3, CD28 and LFA-1 and treated with JAB-1 and cytohesin-1 antagonistic peptides after seven days of culture. We loaded naive CD4⁺ T cells intracellularly with inhibitory or control peptides, stimulated them for three days in plates coated with CD3, CD28 and LFA-1, allowed them to 'rest' for three additional days, restimulated them on day 7, and assessed their intracellular production of IFN- γ and IL-4. The frequency of IFN- γ -producing CD4⁺ T cells decreased in samples treated with the JAB-1 or cytohesin-1 antagonist peptides (Fig. 7d). Therefore, inhibition of LFA-1-mediated pathways reduces the frequency of IFN- γ -producing T_H1 cells that differentiate from naive T cells.

DISCUSSION

Our results show that LFA-1 signaling contributes to CD3 and CD28 costimulation and leads to rapid and optimized naive T cell activation, possibly through a JAB-1-c-Jun- and cytohesin-1-mediated Erk1/2 pathway. This accessory stimulation can, together with CD3 and CD28 and in the absence of additional signals, polarize T cell differentiation toward an apparent T_H1 phenotype. Inhibition of LFA-1 intracellular signaling mechanisms also inhibited the development and frequency of T_H1 cells in long-term culture. Although it is expected that T cell

signaling integrates many additional signals in the native environment, our results show that LFA-1 signaling is an important determinant of phenotypic outcome in naive T cell maturation and effector T cell function.

Initiation of T cell activation requires cell-to-cell contact, an adhesion process mediated mainly by LFA-1. Adhesive events involved in T cell contact have mostly remained unrecognized as transducing signals that may enhance T cell functions. However, there is increasing evidence for the importance of adhesion-mediated events in optimal T cell activation⁵. With a solubilized form of ICAM-2, a normally surface-bound ligand of LFA-1, ICAM-2 binding was able to induce the active form of LFA-1 and induce a calcium influx; we did not find active LFA-1 or induction of a calcium influx with soluble ICAM-1 treatment (O.D.P. and G.P.N., unpublished data). However, plate-bound dimeric ICAM-1 can signal through LFA-1 to induce F-actin reorganization²⁰, indicating that in certain settings, nonsoluble ICAM-1 might signal through LFA-1.

Phosphorylation of β_2 integrin initiated JAB-1 release in a PKC- δ -dependent way as stimulated by LFA-1. Stimulation with phorbol 12-myristate 13-acetate plus ionomycin led to more β_2 integrin phosphorylation than did stimulation with CD3 plus CD28, indicating that additional PKC isozymes may phosphorylate β_2 integrin intracellularly. T cells express several PKC isozymes. It is therefore possible that integration of LFA-1 and TCR signals involves multiple different PKC isozymes. JAB-1 induces phosphorylation of c-Jun⁷ and interacts with several proteins, including p27^{Kip} and MIF-1, and forms part of the COP9 signalsome^{21,22}. Although JAB-1 has been identified as modulating LFA-1-dependent AP-1 gene transcription⁷, its function in T cell activation was not investigated. Here, blocking of JAB-1 inhibited LFA-1-induced c-Jun phosphorylation, thereby disrupting the LFA-1 signal to the AP-1 complex. Additionally, LFA-1 induced

JAB-1 association with p27 in a PKC- δ -dependent way (O.D.P. and G.P.N., unpublished data), indicating that the considerable mitotic progression in LFA-1 stimulation might be invoked by JAB-1 signaling to overcome cell cycle arrest through p27^{Kip} in quiescent T cells. Therefore LFA-1 signaling through JAB-1 may contribute to T cell activation in multiple ways.

Multidimensional analysis of LFA-1 signaling events, in conjunction with stimulation with CD3 plus CD28, showed that naive T cell activation was optimal after triple stimulation. We noted rapid kinetics of IL-2 production in the presence of LFA-1 stimulation that correlated with the early induction of active Erk1/2. CD3, CD28 and LFA-1 signaling produced more activation of Erk1/2 than did CD3 plus CD28 signaling alone 5 min after stimulation. Thus, this important immediate early signal could be essential in T cells for optimal T cell activation. Over several hours, stimulation with CD3 plus CD28 was able to induce Erk1/2, but the presence of the LFA-1 signal gave maximal and optimal results at early time points for Erk1/2 activation and IL-2 production. In support of this idea, T cell lines expressing a constitutively active form of LFA-1 respond to subthreshold stimuli²³, Erk1/2 activation is required for IL-2 expression¹⁸ and thymocytes deficient in p44 show a considerable reduction in proliferation in response to TCR stimulation¹⁷. Early production of IL-2 would also serve as a stimulant for other T cells, as IL-2 stimulation induces Erk1/2 activation²⁴. Furthermore, Erk1/2 activation is required for CD69 and CD25 expression and activation of nuclear factor of activated T cells²⁵, findings in agreement with the results reported here.

Cytohesin-1 regulates LFA-1-mediated adhesion⁸. Transient overexpression of the herpes virus protein kaposin A, which binds cytohesin-1, induced activity of the kinase Erk2 in 293 cells²⁶. Those studies, however, did not determine whether kaposin A-induced Erk2 activity was dependent on cytohesin-1. Our results show that blocking cytohesin-1 function abrogated the LFA-1-induced Erk1/2 activation and inhibited IL-2 production in T cells.

Sustained Erk1/2 activity could be a threshold mechanism for determining partial versus full T cell activation. In experimental models, serial triggering of TCRs results in sustained Erk1/2 activation²⁷, findings that support previous observations that T cells require several hours of stimulation to commit to IL-2 synthesis²⁸. This is in accord with the idea that formation of the immunological synapse allows for full T cell activation through sustained signaling over hours^{18,29}. Indeed, this idea is supported by the kinetic differences between soluble and plate-bound TCR stimulations for many T cell activation proteins, including Erk1/2 activation and the resulting IL-2 production (data not shown). A chief target for Erk1/2 is the transcription factor ELK-1. Activation of ELK-1 is necessary for up-regulation of c-Fos³⁰, so activation of Erk1/2 is in accord with the finding that c-Fos expression was induced after LFA-1 signaling (data not shown). c-Fos dimerizes with c-Jun to form the AP-1 complex, a necessary transcription factor for IL-2 synthesis. Thus, both LFA-1-induced JAB-1-mediated c-Jun phosphorylation and LFA-1-induced cytohesin-1 activation of Erk1/2 converge on components that promulgate AP-1 activity and subsequent IL-2 production. However, this does not exclude the possibility that JAB-1 and cytohesin-1 participate in other signaling events that affect T cell outcomes. Furthermore, AP-1 activity can promote cell cycle progression in several model systems, supporting our results.

The consequences of LFA-1 integrin signaling also induced a polarization of T cells to favor a T_H1 phenotype. CD28 signaling promotes T_H2 differentiation³¹, and blocking interactions of LFA-1 and ICAM favors T_H2 cytokine production³². Inhibiting the Erk1/2 MAPK pathway with pharmacological inhibitors decreases IFN- γ production and enhances IL-4, IL-5 and IL-13 production³³,

findings that indicate the Erk1/2 activity is also involved in effector cell differentiation. Inhibition of Erk1/2 prevents the generation of IFN- γ -producing memory T cells after LFA-1 ligation; however, the mechanisms by which this effect occurred were not investigated³⁴. Inhibiting either JAB-1 or cytohesin-1 decreased the production of IFN- γ -producing T_H1 cells and also the frequency of terminally differentiated T_H1 cells after secondary stimulation. These results indicate functional involvement of LFA-1 in both development and function of T_H1 effector cells, and directly identify key target molecules involved in this process.

LFA-1 signaling can modulate TCR signaling by providing unique signaling events that are independent of TCR signaling, such as those provided through JAB-1, facilitate TCR signaling to achieve a higher threshold of signaling events, such as the integration of cytohesin-1 signaling to Erk1/2 activation, and facilitate the clustering of surface molecules such as the TCR and CD28, and, in turn, enhance critical downstream events. Signaling adapter proteins link TCR signaling to activation of LFA-1 (ref. 35). It is not apparent how each of these molecules contributes to the coordinated orchestration of how the TCR and LFA-1 focus their activities at the immunological synapse, as many of the integrating factors that connect these signaling pathways are not known, although SLAP-130 (SLP-76-associated phosphoprotein) couples TCR to integrin activation and the actin cytoskeleton³⁵. Therefore, the effects of LFA-1 on established TCR signaling molecules, such as CD3, CD28 or possibly others, may be through indirect mechanisms such as cytoskeletal reorganization. Such effects would lower TCR signaling thresholds, if operative. Indeed, adapter proteins SLP-76 and VAV-1 and various GTPases (Rac2, Rac1, RhoA) link TCR signaling to the actin polymerization molecules (Cdc42, WASP and Arp2/3 complex)^{36,37}; disruptions of these block many TCR signaling events, including Erk1/2 activation and actin polymerization^{38–40}. The mechanisms by which LFA-1 integrates into these cytoskeletal-regulated signaling events remains to be determined. Nevertheless, the integration of LFA-1 signaling, whether direct or indirect, promoted more efficient T cell activation than did costimulation with CD3 and CD28 alone *in vitro*.

Inhibition of LFA-1 adhesion by small molecules has shown efficacy in various mouse models of inflammation, but the molecular mechanisms for these results remain unknown. The small molecule BIX 642, an LFA-1 antagonist, inhibited the delayed-type hypersensitivity response in a *trans vivo* (injection of human peripheral blood lymphocytes into the footpads of mice) delayed-type hypersensitivity model⁴¹. An oral LFA-1 inhibitor, LFA703, suppressed the inflammatory response in a murine model of peritonitis⁴². Furthermore, CD18 deficiency in patients, a disease called leukocyte adhesion deficiency, results in severe bacterial infections and can lead to early death^{43–44}. CD18-deficient mice also have severe inflammatory defects, increased susceptibility to *Streptococcus pneumoniae* and a severe defect in leukocyte adhesion and T cell activation⁴⁵. Therefore, the clinical manifestations reported in both patients with leukocyte adhesion deficiency and CD18-deficient mice can confirm the physiological relevance of the signaling function of LFA-1 shown here in T cell activation and effector cell differentiation.

In conclusion, LFA-1 contributed synergistically to naive T cell functionality, as demonstrated by multiple independent assays. This included differences in activated kinase and phosphoproteins, as shown with a flow-based differential assay. LFA-1 signaling through JAB-1 and cytohesin-1 potentially acted in synergy with costimulation with CD3 plus CD28, accelerating several aspects of T cell maturation. In addition, LFA-1 signaling also influenced T_H1 commitment. We expect, given our results, that LFA-1 signaling will be further linked to salient immune cell regulatory events.

METHODS

Immunological and chemical reagents. The following phosphorylated (p-) antibodies were obtained from Cell Signaling Technologies: p-Raf1 (Ser259), p-MEK1/2 (Ser217–221), p-Erk1/2 MAPK (Thr202–Tyr204) monoclonal antibody (mAb), p-Elk-1 (Ser383), p-p38 MAP kinase (Thr180–Tyr182), p-c-Jun (S63), p-AKT (S473), p-PLC- γ 1 (Y783), and p-JNK (T183–185), p-PKC- α/β_{II} (S660), PKC- δ (T505) and PKC- θ (T538). Nonphosphorylation-specific mAbs to those and to Ki-67, JAB-1, PKC isozymes α , β , γ , δ , ϵ , ζ , η , θ , ι , λ and nucleoporin p62 were from Transduction Laboratories. Phosphorylated Erk1/2 (T202–Y204; clone 20a) and phosphorylated p38 (T180–Y182; clone 36) conjugated to Alexa 647, Alexa 488 and phycoerythrin were from BD Biosciences. All surface antibodies, cytokine antibodies and isotype controls were from BD Pharmingen: CD3, CD4, CD8, CD69 and CD25 were conjugated to fluorescein isothiocyanate, phycoerythrin, peridinin chlorophyll protein and allophycocyanin; IL-2, IL-4, IFN- γ were conjugated to fluorescein isothiocyanate and phycoerythrin. Alexa fluor dyes, Cascade blue, Cascade yellow and R-phycoerythrin were from Molecular Probes. Fluorescein isothiocyanate and Texas Red were from Pierce. Indodicarbocyanine (Cy5), bis-functional indodicarbocyanine (Cy5.5) and indotricarbocyanine (Cy7) were from Amersham Life Science. Tandem conjugation protocols for Cy5–phycoerythrin, Cy5.5–phycoerythrin, Cy7–phycoerythrin, Cy5.5–allophycocyanin and Cy7–allophycocyanin can be found at www.drmr.com/abcon. CD102–fluorescein isothiocyanate (ICAM-2) and CD50–phycoerythrin (ICAM-3) were from R&D Systems. DMSO, phorbol 12-myristate 13-acetate, ionomycin, phytohemagglutinin A, propidium iodide and RNase were from Sigma. U0126, PD98059, rottlerin, bisindolymaleimide were from Calbiochem. ICAM-1-FC, ICAM-2-FC, ICAM-3-FC and recombinant human cytokines were from R&D systems. Recombinant PKC isozymes were from Upstate Biotechnologies.

Cell culture, primary cell isolation and cell stimulations. Jurkat T cells (E6.1) were maintained in RPMI-1640 medium supplemented with 5% FCS and 1% PSQ (1,000 units/ml of penicillin and streptomycin and 2mM L-glutamine). The control peptide C-pep1 (MVPRQDRVSY) and Pep24 (MVRYGSSALV) were inserted into retrovirus expression vector pBMN-IRES-GFP at the *Bam*HI and *Sal*I sites, and were produced with the Phoenix Amphi packaging cell line. Jurkat cells were deprived of serum for 12 h for phosphorylation analysis. Human peripheral blood monocytes were obtained by Ficoll-plaque density centrifugation (Amersham Pharmacia) of whole blood from healthy donors (Stanford Blood Bank), and samples were depleted of adherent cells. Primary cells were maintained in complete media (with 5% human sera type AB; Irving Scientific) and were used within 2–4 h of isolation for all stimulations. Magnetic-activated cell sorting was used to enrich for naive CD4 T cells by negative isolation with combinations of CD16, CD14, CD44, HLA-DR, CD8 or CD19 biotinylated antibodies (Dyna) and streptavidin-conjugated magnetic beads (Dyna). Anti-CD3 (clone UCHT1) and anti-CD28 (clone 28.2) were obtained from BD Pharmingen. The mAbs TS1/22 (anti- α) and TS1/18 (anti- β) were from the Developmental Hybridoma Studies Bank. Cells were stimulated in U-bottomed 96-well plates (5 μ g/ml). For cross-linking experiments, 1×10^6 cells were stained at 4 °C with 1 μ g anti-CD3 and 1 μ g anti-CD28. Cells were washed and then subsequently stained for 15 min at 4 °C with 0.5 μ g anti-mouse immunoglobulin G, then were washed and returned to 37 °C for 30 min. Similar cross-linking techniques were used for TS1/22 and TS1/18. The stimulus of CD3 plus CD28 consisted of a 1:1 mixture of CD3 and CD28 (5 μ g/ml each, final concentration). Stimulations for LFA-1 were done with ICAM-2, unless noted otherwise for ICAM-1 or ICAM-3, and LFA-1-specific antibody clones (Fig. 3a).

Kinase assays. MAPK activity was detected with a Erk1/2 MAPK kinase kit as suggested by the manufacturer (Cell Signaling Technologies). PKC kinases assays were done with either recombinant PKC isozymes (Upstate Biotechnologies) or immunopurified PKC isozymes (1 μ g) as suggested by manufacturer of the PKC kinase kits (Upstate Biotechnologies). Biotinylated myelin basic protein or biotinylated β_2 integrin Ser745 substrate (2 μ g) were made to adhere to streptavidin-coated plates (Pierce) and were blocked with 1% BSA. For the radioactive PKC kinase assay, PKC isozymes were immunopurified from Jurkat cells treated for 30 min with ICAM-2 (10 μ g/ml), then immunocomplexes were washed four times with lysis buffer and resuspended in 40 μ l kinase buffer (25 mM Tris, pH 7.5, 5 mM β -glycerolphosphate, 2 mM

DTT, 0.1 mM Na_3VO_4 and 10 mM MgCl_2) supplemented with 200 μ M ATP and 1 μ Ci [γ - ^{32}P]ATP. Samples were then incubated at 37 °C with immunopurified β_2 integrin from Jurkat cells. The kinase reaction was terminated by washing of samples in 'phospho-spin' units (Pierce) in 0.01% phosphoric acid in PBS, and radioactivity was measured by liquid scintillation.

Peptide synthesis, affinity-binding assay and phosphopeptide analysis. Biotinylated peptides that correspond to the β_2 integrin chain residues 740–750 (β_2 -pep745; CKEKLKSQWNND-biotin) and residues 750–761 (β_2 -pep756; (CNPLFKSATTTV-biotin) were synthesized by F-moc solid-phase peptide synthesis (Biosource International). Cell-permeable peptides for cytohesin-1 dominant negative peptide (AARKKKVSTKRGSRRRRRR), JAB-1 antagonist peptide Pep24 (MVRYGSSALV-GSRRRRRR) and control peptide C-pep1 (MVPRQDRVSY-GSRRRRRR)^{46–49} were synthesized by Invitrogen. A human immunodeficiency virus Tat peptide (amino acids 48–60; GRKKR-RQRQ) was used as control carrier. The PKC- δ agonist (RQRKKRG-CC-MRAAEDPM) and PKC- δ antagonist (RQRKKRG-CC-SFBSYELGSL) peptides were synthesized as described¹². Peptides were purified by HPLC to >98% purity, and sequences were verified by mass spectrometry. β_2 -pep745 and β_2 -pep756 were phosphorylated by incubation of 10 μ g peptide with 0.1 μ g recombinant PKC- α in kinase buffer (described above). Phosphopeptides were separated by phosphocellulose spin columns (Pierce) and eluted with 0.5 mM KCl. Biotinylated phosphopeptides and non-phosphopeptides were incubated for 15 min with streptavidin-coupled magnetic beads (Pierce), washed twice in PBS by magnetic separation, and incubated for 1 h at 4 °C with constant rotation with 100 μ g of lysates of CD4⁺ T cells in 1 ml PBS with 4% FCS. The streptavidin-peptide complexes were separated with a magnetic particle separator (Dyna), washed twice in PBS and boiled in sample buffer.

Flow cytometry. Peripheral blood mononuclear cells (1×10^7 to 1×10^8 nonactivated CD4⁺ T cells) were magnetically sorted (negative isolation), treated with a stimulus and prepared for flow cytometry. Brefeldin A (10 μ g/ml) was added for intracellular cytokine detection for 6 h (or as indicated in Fig. 6b). Intracellular probes for active kinases were made as described⁹. For multiparameter surface and intracellular staining, cells were seeded into 96 wells 12 h before stimulation, and intracellular phosphorylation staining was done by washing cells in buffer A (PBS, pH 7.4, 0.5 mM EDTA, 1 mM β -glycerolphosphate, 1 mM Na_3VO_4 , 1 μ g/ml of microcystin, 1 μ g/ml of leupeptin and a protease inhibitor 'cocktail' tablet), surface-staining them in buffer B (5% FCS and 1 mM NaN_3 in buffer A), fixing them in buffer C (1% paraformaldehyde in buffer A), permeabilizing them in buffer D (0.2% saponin (25% saponigen content) and 5% FCS in buffer A) and resuspending them in buffer E (PBS with 0.5 mM EDTA). Cells were washed twice in PBS (with 1 mM β -glycerolphosphate, 1 mM Na_3VO_4 , 1 μ g/ml of microcystin, 1 μ g/ml of leupeptin and a protease inhibitor 'cocktail' tablet) between stains (15 min surface; 30 min intracellular) and fixation (15 min). For detection of phosphorylated β_2 integrin and phosphorylated c-Jun, cells were stimulated, fixed (2% paraformaldehyde, 15 min) and permeabilized with ice-cold methanol (15 min). Kinetic analyses were done by direct application of fixation buffer in 'time-synchronized' 96 wells maintained at 37 °C. Then, 200 μ l of 2% paraformaldehyde was added to 100 μ l stimulated cells (0.5×10^6) and samples were pipetted up and down three times in a 37 °C water bath and fixed for 10 min at 37 °C, and then plates were centrifuged at 500g for 5 min at 4 °C and stained. Four-color (or less) flow cytometry data acquisition was made with a FACSCalibur machine (Becton Dickinson) with CELLQuest software, analyzed and presented with FlowJo software (Tree Star). The 11-color data acquisition was made with a modified FACStarPlus (Becton Dickinson) connected to MoFlo electronics (Cytomation). Data were collected by FACS-Desk software and compensated, analyzed and presented with FlowJo software. Phosphorylated kinase clustering analysis was done by inputting of fluorescence intensity values (geometric means) of flow cytometric staining into Cluster and Treeview programs. All quantification of fluorescence intensity values for intracellular stains was obtained by computation of the geometric mean.

Cytometric bead arrays were from BD Pharmingen. Ratios for secreted cytokines by CBA were calculated from the following equation (MFI is median fluorescent intensity): $[(\text{MFI}_{\text{Experimental cytokine1}} - \text{MFI}_{\text{Control cytokine1}}) / (\text{MFI}_{\text{Experimental cytokine2}} - \text{MFI}_{\text{Control cytokine2}})]$, where 'experimental' is a treated

sample and 'control' is an untreated sample. All CBA measurements were quantified with the median fluorescence values. Ratios of intracellular flow cytometric measurements were calculated with geometric mean values from the following equation: $\text{Log} [(GMFI_{\text{Experimental}} - GMFI_{\text{Isotype mAb}}) / (GMFI_{\text{Control}} - GMFI_{\text{Isotype mAb}})]$, where geometric mean fluorescent intensity values (GMFI) are used.

Urls. A more complete description of these procedures can be found in the **Supplementary Methods** online or at <http://www.stanford.edu/group/nolan/protocols/phosphofacs/OP/NIMatMethods.html>.

Note: Supplementary information is available on the Nature Immunology website.

ACKNOWLEDGMENTS

We acknowledge support from BD Biosciences-Pharmingen and the Baxter Foundation; and D. Parks and the Herzenberg Laboratory for the resources of the Stanford FACS facility. We thank N. Hogg for mAb 24; J.F. Fortin for the NFAT-luciferase-transfected cells; and C.C. Gahmberg for the gift of phosphorylated β_2 integrin antibodies. We thank I. Weissman, M. Davis, H. Blau and R. Smith for discussions; G. Fathman for review of this manuscript; and K. Vang for administrative help. O.D.P. was supported by the Bristol-Meyer Squibb Irvington Institute and the National Heart, Lung and Blood Institute (N01-HV-281831). G.P.N. was supported by the National Institutes of Health (P01-AI39646, AR44565, AI35304, N01-AR-6-2227, A1/GF41520-01), the National Heart, Lung and Blood Institute (N01-HV-281831) and the Juvenile Diabetes Foundation.

COMPETING INTERESTS STATEMENT

The authors declare that they have no competing financial interests.

Received 8 May; accepted 4 September 2003

Published online at <http://www.nature.com/natureimmunology/>

- Norcross, M.A. A synaptic basis for T-lymphocyte activation. *Ann. Immunol. (Paris)* **135D**, 113–134 (1984).
- Lenschow, D.J., Walunas, T.L. & Bluestone, J.A. CD28/B7 system of T cell costimulation. *Annu. Rev. Immunol.* **14**, 233–258 (1996).
- Abraham, C., Griffith, J. & Miller, J. The dependence for leukocyte function-associated antigen-1/ICAM-1 interactions in T cell activation cannot be overcome by expression of high density TCR ligand. *J. Immunol.* **162**, 4399–4405 (1999).
- Ragazzo, J.L., Ozaki, M.E., Karlsson, L., Peterson, P.A. & Webb, S.R. Costimulation via lymphocyte function-associated antigen 1 in the absence of CD28 ligation promotes energy of naive CD4⁺ T cells. *Proc. Natl. Acad. Sci. USA* **98**, 241–246 (2001).
- Wulfing, C., Sjaastad, M.D. & Davis, M.M. Visualizing the dynamics of T cell activation: intracellular adhesion molecule 1 migrates rapidly to the T cell/B cell interface and acts to sustain calcium levels. *Proc. Natl. Acad. Sci. USA* **95**, 6302–6307 (1998).
- Rovere, P., Inverardi, L., Bender, J.R. & Pardi, R. Feedback modulation of ligand-engaged $\alpha_L\beta_2$ leukocyte integrin (LFA-1) by cyclic AMP-dependent protein kinase. *J. Immunol.* **156**, 2273–2279 (1996).
- Bianchi, E. *et al.* Integrin LFA-1 interacts with the transcriptional co-activator JAB1 to modulate AP-1 activity. *Nature* **404**, 617–621 (2000).
- Kolanus, W. *et al.* $\alpha_L\beta_2$ integrin/LFA-1 binding to ICAM-1 induced by cytohesin-1, a cytoplasmic regulatory molecule. *Cell* **86**, 233–242 (1996).
- Perez, O.D. & Nolan, G.P. Simultaneous measurement of multiple active kinase states using polychromatic flow cytometry. *Nat. Biotechnol.* **20**, 155–162 (2002).
- Hogg, N. *et al.* Mechanisms contributing to the activity of integrins on leukocytes. *Immunol. Rev.* **186**, 164–171 (2002).
- Fagerholm, S., Morrice, N., Gahmberg, C.G. & Cohen, P. Phosphorylation of the cytoplasmic domain of the integrin CD18 chain by protein kinase C isoforms in leukocytes. *J. Biol. Chem.* **277**, 1728–1738 (2002).
- Chen, L. *et al.* Opposing cardioprotective actions and parallel hypertrophic effects of δ PKC and ϵ PKC. *Proc. Natl. Acad. Sci. USA* **98**, 11114–11119 (2001).
- Weber, K.S. *et al.* Cytohesin-1 is a dynamic regulator of distinct LFA-1 functions in leukocyte arrest and transmigration triggered by chemokines. *Curr. Biol.* **11**, 1969–1974 (2001).
- Dierks, H., Kolanus, J. & Kolanus, W. Actin cytoskeletal association of cytohesin-1 is regulated by specific phosphorylation of its carboxyl-terminal polybasic domain. *J. Biol. Chem.* **276**, 37472–37481 (2001).
- Zola, H. Markers of cell lineage, differentiation and activation. *J. Biol. Regul. Homeost. Agents* **14**, 218–219 (2000).
- Yu, T.K., Caudell, E.G., Smid, C. & Grimm, E.A. IL-2 activation of NK cells: involvement of MKK1/2/ERK but not p38 kinase pathway. *J. Immunol.* **164**, 6244–6251 (2000).
- Pages, G. *et al.* Defective thymocyte maturation in p44 MAP kinase (Erk 1) knockout mice. *Science* **286**, 1374–1377 (1999).
- Koike, T. *et al.* A novel ERK-dependent signaling process that regulates interleukin-2 expression in a late phase of T cell activation. *J. Biol. Chem.* **278**, 15685–15692 (2003).
- Murphy, K.M. *et al.* Signaling and transcription in T helper development. *Annu. Rev. Immunol.* **18**, 451–494 (2000).
- Porter, J.C., Bracke, M., Smith, A., Davies, D. & Hogg, N. Signaling through integrin LFA-1 leads to filamentous actin polymerization and remodeling, resulting in enhanced T cell adhesion. *J. Immunol.* **168**, 6330–6335 (2002).
- Tomoda, K. *et al.* The cytoplasmic shuttling and subsequent degradation of p27Kip1 mediated by Jab1/CNS5 and the COP9 signalosome complex. *J. Biol. Chem.* **277**, 2302–2310 (2002).
- Kleemann, R. *et al.* Intracellular action of the cytokine MIF to modulate AP-1 activity and the cell cycle through Jab1. *Nature* **408**, 211–216 (2000).
- Damle, N.K. *et al.* Costimulation via vascular cell adhesion molecule-1 induces in T cells increased responsiveness to the CD28 counter-receptor B7. *Cell. Immunol.* **148**, 144–156 (1993).
- Kovanen, P.E. *et al.* Analysis of γ c-family cytokine target genes. Identification of dual-specificity phosphatase 5 (DUSP5) as a regulator of mitogen-activated protein kinase activity in interleukin-2 signaling. *J. Biol. Chem.* **278**, 5205–5213 (2003).
- Villalba, M., Hernandez, J., Deckert, M., Tanaka, Y. & Altman, A. Vav modulation of the Ras/MEK/ERK signaling pathway plays a role in NFAT activation and CD69 up-regulation. *Eur. J. Immunol.* **30**, 1587–1596 (2000).
- Kliche, S. *et al.* Signaling by human herpesvirus 8 kaposin A through direct membrane recruitment of cytohesin-1. *Mol. Cell* **7**, 833–843 (2001).
- Borovsky, Z., Mishan-Eisenberg, G., Yaniv, E. & Rachmilewitz, J. Serial triggering of T cell receptors results in incremental accumulation of signaling intermediates. *J. Biol. Chem.* **277**, 21529–21536 (2002).
- Weiss, A., Shields, R., Newton, M., Manger, B. & Imboden, J. Ligand-receptor interactions required for commitment to the activation of the interleukin 2 gene. *J. Immunol.* **138**, 2169–2176 (1987).
- Dustin, M.L. Coordination of T cell activation and migration through formation of the immunological synapse. *Ann. NY Acad. Sci.* **987**, 51–59 (2003).
- Li, W. *et al.* CD28 signaling augments Elk-1-dependent transcription at the c-fos gene during antigen stimulation. *J. Immunol.* **167**, 827–835 (2001).
- Glimcher, L.H. & Murphy, K.M. Lineage commitment in the immune system: the T helper lymphocyte grows up. *Genes Dev.* **14**, 1693–1711 (2000).
- Salomon, B. & Bluestone, J.A. LFA-1 interaction with ICAM-1 and ICAM-2 regulates Th2 cytokine production. *J. Immunol.* **161**, 5138–5142 (1998).
- Dumont, F.J., Staruch, M.J., Fischer, P., DaSilva, C. & Camacho, R. Inhibition of T cell activation by pharmacologic disruption of the MEK1/ERK MAP kinase or calcineurin signaling pathways results in differential modulation of cytokine production. *J. Immunol.* **160**, 2579–2589 (1998).
- Smits, H.H. *et al.* Interleukin adhesion molecule-1/LFA-1 ligation favors human Th1 development. *J. Immunol.* **168**, 1710–1716 (2002).
- Peterson, E.J. *et al.* Coupling of the TCR to integrin activation by Slap-130/Fyb. *Science* **293**, 2263–2265 (2001).
- Griffiths, E.K. & Penninger, J.M. Communication between the TCR and integrins: role of the molecular adapter ADAP/Fyb/Slap. *Curr. Opin. Immunol.* **14**, 317–322 (2002).
- Griffiths, E.K. & Penninger, J.M. ADAP-ting TCR signaling to integrins. *Sci. STKE* **2002**, RE3 (2002).
- Krawczyk, C. *et al.* Vav1 controls integrin clustering and MHC/peptide-specific cell adhesion to antigen-presenting cells. *Immunity* **16**, 331–343 (2002).
- Costello, P.S. *et al.* The Rho-family GTP exchange factor Vav is a critical transducer of T cell receptor signals to the calcium, ERK, and NF- κ B pathways. *Proc. Natl. Acad. Sci. USA* **96**, 3035–3040 (1999).
- Yu, H., Leitenberg, D., Li, B. & Flavell, R.A. Deficiency of small GTPase Rac2 affects T cell activation. *J. Exp. Med.* **194**, 915–926 (2001).
- Winquist, R.J. *et al.* The role of leukocyte function-associated antigen-1 in animal models of inflammation. *Eur. J. Pharmacol.* **429**, 297–302 (2001).
- Weitz-Schmidt, G. *et al.* Statins selectively inhibit leukocyte function antigen-1 by binding to a novel regulatory integrin site. *Nat. Med.* **7**, 687–692 (2001).
- Hogg, N. *et al.* A novel leukocyte adhesion deficiency caused by expressed but non-functional β_2 integrins Mac-1 and LFA-1. *J. Clin. Invest.* **103**, 97–106 (1999).
- Anderson, D.C. & Springer, T.A. Leukocyte adhesion deficiency: an inherited defect in the Mac-1, LFA-1, and p150,95 glycoproteins. *Annu. Rev. Med.* **38**, 175–194 (1987).
- Scharfetter-Kochanek, K. *et al.* Spontaneous skin ulceration and defective T cell function in CD18 null mice. *J. Exp. Med.* **188**, 119–131 (1998).
- Schwarze, S.R., Ho, A., Vocero-Akbani, A. & Dowdy, S.F. *In vivo* protein transduction: delivery of a biologically active protein into the mouse. *Science* **285**, 1569–1572 (1999).
- Schwarze, S.R., Hruska, K.A. & Dowdy, S.F. Protein transduction: unrestricted delivery into all cells? *Trends Cell Biol.* **10**, 290–295 (2000).
- Wender, P.A. *et al.* The design, synthesis, and evaluation of molecules that enable or enhance cellular uptake: peptidic molecular transporters. *Proc. Natl. Acad. Sci. USA* **97**, 13003–13008 (2000).
- Rothbard, J.B. *et al.* Arginine-rich molecular transporters for drug delivery: role of backbone spacing in cellular uptake. *J. Med. Chem.* **45**, 3612–3618 (2002).

Erratum: Leukocyte functional antigen 1 lowers T cell activation thresholds and signaling through cytohesin-1 and Jun-activating binding protein 1

Omar D Perez, Dennis Mitchell, Gina C Jager, Sharon South, Chris Murriel, Jacqueline McBride, Lee A Herzenberg, Shigemi Kinoshita & Garry P Nolan

Nature Immunology 4, 1083–1092 (2003).

On page 1083, the fourth line of the main text should read "...LFA-1, also known as CD11a-CD18, and the intercellular...". On page 1084, 10 lines from the bottom of the second column, the PKC isoenzymes should be identified with Greek letters to read "recombinant human PKC isozymes α , β , γ , δ , ϵ , η , θ , ι and λ ." On page 1085, four lines from the bottom of column 2, the authors of the unpublished data should be identified as "S.K., O.D.P. and G.P.N." On page 1086, six lines from the bottom of column 2 the third molecule listed should be pLck. Finally, on page 1091, in column 2, first full paragraph, the sequences of the cell-permeable peptides should not be underlined. *Nature Immunology* regrets these errors.